Parasitology

cambridge.org/par

Quantitative monitoring of experimental and human leishmaniasis employing amastigote-specific genes

Madhurima Roy, Deblina Sarkar and Mitali Chatterjee

Department of Pharmacology, Institute of Postgraduate Medical Education and Research (IPGME&R), 244B, Acharya JC Bose Road, Kolkata 700020, India

Research Article

Cite this article: Roy M, Sarkar D, Chatterjee M (2022). Quantitative monitoring of experimental and human leishmaniasis employing amastigote-specific genes. *Parasitology* **149**, 1085–1093. https://doi.org/10.1017/S0031182022000610

Received: 31 January 2022
Revised: 26 April 2022
Accepted: 26 April 2022
First published online: 10 May 2022

Key words:
A2; amastigotes; *amastin*; droplet digital polymerase chain reaction (ddPCR); post kala-azar dermal leishmaniasis (PKDL)

Author for correspondence:
Mitali Chatterjee, E-mail: ilatimc@gmail.com

Abstract

The gold standard for diagnosis of leishmaniasis is the microscopic detection of amastigotes/Leishman Donovan (LD) bodies, but its moderate sensitivity necessitates the development of molecular approaches. This study aimed to quantify in experimental animal models and human leishmaniasis the expression of amastigote-specific virulence genes, *A2* and *amastin* by droplet digital polymerase chain reaction (ddPCR). Total RNA was isolated from *L. donovani*-infected hamsters or murine peritoneal macrophages and lesional biopsies from patients with post kala-azar dermal leishmaniasis (PKDL). Following cDNA conversion, EvaGreen-based ddPCR was performed using specific primers for *A2* or *amastin* and parasite load expressed in copies per μL. Assay was optimized and the specificity of amastigote-specific *A2* and *amastin* was confirmed. In hepatic and splenic tissues of *L. donovani*-infected hamsters and peritoneal macrophages, ddPCR demonstrated a greater abundance of *A2* than *amastin*. Treatment of *L. donovani*-infected peritoneal macrophages with conventional anti-leishmanials, miltefosine and amphotericin B translated into a dose-dependent reduction in copies per μL of *A2* and *amastin*, and the extrapolated IC_{50} was comparable with results obtained by counting LD bodies in Giemsa-stained macrophages. Similarly, in dermal biopsies of patients with PKDL, *A2* and *amastin* were detected. Overall, monitoring of *A2* by ddPCR can be an objective measure of parasite burden and potentially adaptable into a high throughput approach necessary for drug development and monitoring disease progression when the causative species is *L. donovani*.

Introduction

Leishmaniasis is caused by the digenetic parasite *Leishmania* which are flagellated promastigotes within the sandfly vector and aflagellated amastigotes within susceptible host macrophages (Sunter and Gull, 2017; Bates, 2018). Leishmaniasis has a diverse disease spectrum that ranges from a self-limiting cutaneous lesion to the fatal form of visceral leishmaniasis (VL), while has a dermal sequel, post kala-azar dermal leishmaniasis (PKDL; Chappuis *et al.*, 2007; Zijlstra *et al.*, 2017; Gedda *et al.*, 2020). The study of human leishmaniasis is facilitated using Syrian golden hamsters as it shares pathological features and immunological responses comparable with humans (Melby *et al.*, 2001; Garg and Dube, 2006; Saini and Rai, 2020; Moulik *et al.*, 2021*a*).

Animal models are an invaluable resource to screen for potential anti-leishmanials using *in vivo*/*ex vivo* approaches (Vermeersch *et al.*, 2009). Generally, the initial screening is in *Leishmania*-infected macrophages and the number of amastigotes in host cells is a direct measure of drug activity (Escobar *et al.*, 2002; Yardley *et al.*, 2005). This requires microscopic counting and being a subjective approach, is susceptible to operator bias. To obviate this subjectivity, molecular approaches are the need of the hour and preferably those that can identify amastigotes.

A molecular target should have high abundance and this criterion is best achieved by kinetoplast mini-circle DNA (kDNA), present as 1000 copies per cell in all *Leishmania* spp. (Salotra *et al.*, 2001; Mary *et al.*, 2004). In fact, the kDNA-based qPCR or real-time PCR has stood the test of time in determining parasite load (Mary *et al.*, 2006; Verma *et al.*, 2010; Sudarshan *et al.*, 2011; Abbasi *et al.*, 2013; Hossain *et al.*, 2017; Moulik *et al.*, 2018, 2021*b*). However, for *ex vivo* drug screening, there is no assay that can selectively detect amastigotes, reflecting the need to further optimize molecular methods of detection.

In terms of amastigote-specific genes, the most well studied is the *A2* gene family first identified in *L. donovani* amastigotes translating into a family of A2 proteins ranging from 45 to 100 kDa (Charest and Matlashewski, 1994; Avishek *et al.*, 2018). The A2 protein is also expressed at high levels in axenic amastigotes (Matlashewski, 2001). Another important amastigote-specific gene is *amastin* present as a surface protein (Johnston *et al.*, 1999). It contains a unique, highly conserved 11-amino acid signature at the N terminus. The presence of *amastin* has been reported in *Trypanosoma cruzi* (McCall and Matlashewski, 2010) and *Leishmania infantum* amastigotes (Rochette *et al.*, 2005). The latex agglutination test (LAT), a rapid diagnostic test for detection of anti-*Leishmania* antibodies, utilizes the A2 antigen and exhibited accuracy comparable to direct agglutination test (Akhoundi *et al.*, 2013). The

CAMBRIDGE UNIVERSITY PRESS

amastigote-derived A2 protein has also been investigated for antibody responses in India, Sudan and South America with variable sensitivities (Carvalho *et al.*, 2002). Similarly, amastin peptides have been employed for the serodiagnosis of active VL (Rafati *et al.*, 2006).

The droplet digital polymerase chain reaction (ddPCR) detects samples with a low copy number of the target nucleic acid and additionally allows direct quantification without the need for a standard curve (Belmonte *et al.*, 2016). The traditional qPCR uses an analogue approach as it quantifies samples by comparing their cycle threshold (C_t) to a standard curve generated by well-defined samples. However, development of such a standard curve for detection of amastigotes is challenging as they are present within host macrophages and it is not feasible to quantify the exact burden of amastigotes per macrophage. The advent of the analytical ddPCR assay and it not requiring a standard curve makes it a value addition in the field of nucleic acid quantification (Gobert *et al.*, 2018). The principle for ddPCR is based on the reaction mixture being divided into hundreds to millions of partitions (droplets in oil emulsion), and each droplet being capable of initiating an independent PCR reaction. At the end-point, the partitions are scored as positive or negative and these values are used to calculate the target concentration using binomial Poisson statistics (Pinheiro *et al.*, 2012). Using statistical software, the target gene copy number is automatically determined based on the number of droplets positive for amplification of the target nucleic acid (Cai *et al.*, 2014; Floren *et al.*, 2015). In view of limited molecular assays to quantify the disease burden in terms of amastigotes, this study aimed to develop a ddPCR-based semi-automated approach for quantifying the expression of amastigote-specific genes *A2* and *amastin* adaptable for parasitological detection in (i) drug screening assays and (ii) PKDL.

Materials and methods

Reagents

All reagents were of analytical grade and obtained from Bio-Rad Laboratories (Hercules, CA, USA) and Sigma-Aldrich (St. Louis, MO, USA), except cDNA Reverse Transcription kit and SYBR Green Quantitative PCR (qPCR) Master Mix from Applied Biosystems (Grand Island, NY, USA), Trizol reagent and RNA*Later* (Ambion, Austin, TX, USA) and fetal bovine serum (FBS, Gibco, Thermo Fischer Scientific, Waltham, MA, USA).

Parasite culture

Leishmania donovani (MHOM/IN/1983/AG83) promastigotes were maintained at 24°C in M199 medium supplemented with 10% heat-inactivated FBS, penicillin G (50 IU mL^{-1}) and streptomycin (50 $\mu g\ mL^{-1}$); parasites were sub-cultured every 48–72 h, inoculum being 1×10^6 cells mL^{-1}.

Experimental models of visceral leishmaniasis

Hepatic and splenic tissues were obtained from *L. donovani*-infected male golden hamsters (*Mesocricetus auratus*, 45–50 g, $n = 10$) maintained in the Division of Parasitology, Central Drug Research Institute (CDRI), Lucknow, India, and kindly provided by Dr Anuradha Dube, CDRI, Lucknow. Tissue samples were stored in RNA*Later* at −80°C.

Peritoneal macrophages were isolated from male/female Swiss albino mice (6–10 weeks old, 20–25 g) housed in the animal facility, IPGME&R, Kolkata, India under controlled temperature (22 ± 5°C), humidity (60 ± 5%) and a 12 h light/dark cycle. Stationary 5–7 days old promastigote cultures were used for *ex vivo* infection. Briefly, following an IP administration of 10–15 mL chilled phosphate-buffered saline (0.02 M phosphate, pH 7.2, PBS), the peritoneal exudate was aspirated and resuspended in RPMI medium (Phenol Red+) supplemented with 10% FBS, penicillin G (50 IU mL^{-1}) and streptomycin (50 $\mu g\ mL^{-1}$).

The peritoneal exudate was seeded ($\sim 2 \times 10^6\ mL^{-1}$) in 12-well plates; following an overnight incubation (37°C, 5% CO_2), the non-adherent cells were removed and adherent macrophages infected with stationary phase promastigotes at a multiplicity of infection of 10:1 (parasite: macrophage) for 48 h (Karmakar *et al.*, 2019). Subsequently, anti-leishmanials, miltefosine (HePC, 0–5 μM) or amphotericin B (AmphoB, 0–50 nM) were added and after an additional 48 h, the cells were recovered by gentle scraping, and the cell pellets stored in RNA*Later* at −80°C. Alongside, infected peritoneal macrophages with and without drug treatments were stained with Giemsa and independently examined in a blinded manner under a bright-field light microscope (EVOS FL Cell Imaging System, Waltham, MA, USA), the % infectivity and number of intracellular amastigotes was counted in at least 100 macrophages/slide.

Study population

Patients with a clinical diagnosis of PKDL ($n = 10$) were recruited either from Dermatology Outpatient Departments of School of Tropical Medicine/Calcutta Medical College/IPGME&R, Kolkata or from active field surveys conducted in endemic districts of West Bengal (Malda, Dakshin Dinajpur, Murshidabad and Birbhum) by a camp approach, using standard case definitions and defined risk factors, for example, living in an endemic area and having an epidemiological link (past history of VL). The diagnosis of PKDL was primarily based on clinical features and a history of VL, rK-39 strip test positivity and/or confirmed by demonstration of LD bodies by Giemsa staining, and/or ITS-1 PCR (Sengupta *et al.*, 2019). Informed consent was taken for a 4 mm punch biopsy. Cases with hypopigmented macules were considered as macular PKDL, whereas an assortment of papules, nodules, macules and/or plaques was termed as polymorphic PKDL. None suffered from any co-infection or pre-existing disease, and pregnant women were excluded. Samples were collected at disease presentation. For controls, skin biopsies ($n = 10$) from foreskin of males undergoing voluntary circumcision were obtained. Dermal biopsies were stored in RNA*Later* at −80°C.

Optimization and determination of copy number of target genes using droplet digital PCR

The assay was performed using total RNA isolated by the Trizol method from *Leishmania*-infected murine peritoneal macrophages, hepatic or splenic tissues from hamsters ($n = 10$) and dermal biopsies of patients with PKDL ($n = 10$). The concentration of RNA was measured in Nanodrop™ One/One^C Microvolume UV-Vis Spectrophotometer (Thermo Fischer Scientific, MA, USA) and converted to single-stranded cDNA using the High-Capacity cDNA Reverse Transcription Kit (Applied Biosystems™, MA, USA), according to the manufacturer's instructions. The final concentration of prepared cDNA was 1 μg (for a 20 μL reaction) and detection of amplicons was done using primers (sourced from NCBI Primer – BLAST, https://www.ncbi.nlm.nih.gov/tools/primer-blast) whose specificity was confirmed by UCSC In-Silico PCR for amastigote-specific genes *A2* (F, 5′-CTGCAGGCTGTT GACGTTTC-3′; R, 5′-AAGGTTTGCCTCGTCACCAT-3′) and *amastin* (F, 5′-GTGCATCGTGTTCATGTTCC-3′; R, 5′GGGC GGTAGTCGTAATTGTT-3′). Absolute quantification was performed by ddPCR using primers for *A2* and *amastin*, and expression determined as copies per μL using QuantaSoft software (version 1.7.4, Bio-Rad Laboratories).

https://doi.org/10.1017/S0031182022000610 Published online by Cambridge University Press

Briefly, the optimized reaction mixture containing cDNA (50 ng) was added to a ddPCR EvaGreen Supermix (Bio-Rad Laboratories, CA, USA) containing 100 nM mL^{-1} of each forward and reverse primer, final volume being 20 μL. For negative controls (NC), 10 μL nuclease-free water was added along with 10 μL of ddPCR Eva Green Super mix, and in case of non-template control (NTC), nuclease-free water was used instead of cDNA. Each reaction was then loaded into a sample well of an 8-well disposable cartridge (DG8), along with 70 μL of droplet generation oil. Droplets were formed using QX200 droplet generators which were then transferred to a 96-well PCR plate to perform PCR of 40 cycles at 95°C for 5 min, 95°C for 30 s, annealing (58–62°C) for 1 min, with a final extension at 90°C for 5 min. In ddPCR, the reaction mixture is partitioned into tens of thousands of droplets, with each droplet being an independent PCR reaction. The target template copy number is determined based on the number of droplets positive for amplification of the target template and these values help to calculate the target concentration using binomial Poisson statistics (Pinheiro *et al.*, 2012). The resultant products were scanned on a QX200 Droplet Reader, and data analysed using QuantaSoft software (version 1.7.4, Bio-Rad Laboratories; Dighal *et al.*, 2020) and expressed as copies per μL with confidence intervals of 95%. The threshold was adjusted based on clear demarcation of positive droplets from the negative cluster with respect to individual wells (Supplementary Fig. S1). The background signals were eliminated using an NC and NTC.

Optimization of ddPCR reaction conditions was performed with (a) varying amounts of target cDNA obtained from infected liver and splenic tissues of hamsters (12.5–100 ng), (b) annealing temperature (58–62°C) and (c) primer concentration (100–500 nM mL^{-1}). The optimal expression of 6.0 and 1.8 copies μL^{-1} for *A2* and *amastin*, respectively, was detected with 50 ng template, 100 nM mL^{-1} of primer, Tm at 58°C (Supplementary Figs S2–S4 and Table S1). A dramatic drop in expression was observed when the template concentration was 100 ng μL^{-1}, attributable to excess of template causing inhibition of PCR reaction. Additionally, with increasing concentration of template, there may be exhaustion of products like oligos, primer/probe, etc., accounting for the drop in signal amplification. It may also result in the formation of packed DNA structures within the confined space of the reaction tube, thereby increasing the chance of false priming and cause a poor yield (https://www.caister.com/highveld/pcr/pcr-troubleshooting). These standardized parameters were considered as optimal conditions and subsequently, the detection of amastigote load was performed.

Controls for droplet digital PCR

Both NC and NTC were used to define the cut-off. NC, i.e. template negative for amplification by *A2* and *amastin*, included (i) uninfected hepatic and splenic tissues, (ii) uninfected peritoneal macrophages, (iii) preputial skin biopsies from males undergoing voluntary circumcision and (iv) promastigotes. NTC included the use of nuclease-free water as template.

Determination of the cut-off for droplet digital PCR

The ddPCR assay determined NTC as 'No Call' with a single threshold line for *A2* and *amastin* based on no copies detected using the QuantaSoft™ software (black droplets). Samples were marked as positive (blue droplets) if more than 4 fluorescent signal events were shown above the threshold line to avoid false positivity. The cut-off for the ddPCR assay was defined based on negative samples as they did not show more than 2 fluorescent signals. The assay sensitivity was validated by determining the absolute limit of detection (aLOD), i.e. the lowest target copy number in a sample that can be reliably detected, but not necessarily quantified. The absolute limit of quantification (aLOQ) is the lowest target copy number in a sample that can be reliably quantified with an acceptable level of precision and accuracy (Holst-Jensen *et al.*, 2003); in ddPCR, the aLOQ was equivalent to aLOD. The sensitivity of the performed assay was evaluated by the receiver operating characteristic (ROC) curve and area under the ROC curve (AUC) values with 95% confidence interval. The linearity of the optimized ddPCR assay was determined and the linear regression was established as R^2; values >0.7 were considered as a strong and effective coefficient parameter.

Measurement of parasite load by real-time polymerase chain reaction (qPCR)

DNA extraction was performed according to the manufacturer's instructions (QIAamp DNA Mini Kit, Qiagen, NW, Germany) from tissue biopsies collected in phosphate-buffered saline (20 mM, pH 7.4), excised into small pieces and eluted in 50 μL of DNA elution buffer. For measurement of parasite load in hepatic and splenic tissues sourced from infected hamsters and in patients with PKDL, a standard curve was generated and real-time PCR was performed (Ghosh *et al.*, 2015; Moulik *et al.*, 2018). The parasite number when <10 reported a cycle threshold (C_t) value almost equivalent to NTC, and was accorded an arbitrary value of 1.

Statistical analysis

Data were analysed either by Mann–Whitney *t* test (in case of 2 groups) and Kruskal–Wallis test (more than 2 groups) for non-parametric data using GraphPad Prism software version 8.4.2 (GraphPad Software, La Jolla, California, USA), $P < 0.05$ was considered significant. ddPCR data were expressed as mean ± S.E.M. (standard error of mean). Correlation was calculated using Pearson's correlation and the coefficient of correlation (r) when >0.4 was considered as relevant.

Results

Measurement of parasite load

The parasite load was measured in *Leishmania*-infected hamsters by qPCR using specific primers for minicircle kDNA and was quantified using a standard curve. During the initial phase of *Leishmania* infection, parasites rapidly multiply both in the liver and spleen, but the latter demonstrates a higher parasite burden upon establishment of infection (Moreira *et al.*, 2012; Moulik *et al.*, 2021*a*). This was reflected in this study as the parasite load in hepatic and splenic tissues was 6512 (4369–9957) and 60 982 (48 862–85 820) parasites per μg of genomic DNA, respectively.

Measurement of amastigote-specific genes in animal models of visceral leishmaniasis

In liver tissues from infected hamsters, the expression of *A2* was detected as compared to their uninfected counterparts, being 2.42 ± 0.38 *vs* 0.01 ± 0.00 copies μL^{-1}, $P < 0.001$ (Fig. 1A, i, iii). Similarly, in splenic tissues, *A2* was substantially raised being 12.15 ± 3.62 *vs* 0.02 ± 0.00 copies μL^{-1} (Fig. 1A, ii, v). Importantly, *A2* correlated positively with parasite load, in hepatic ($r = 0.87$) and splenic ($r = 0.87$) tissues (Fig. 1A, iv, vi). With regard to *amastin*, it was raised in liver and splenic tissues, being 1.61 ± 0.17 *vs* 0.01 ± 0.01 copies μL^{-1}, $P < 0.001$ (Fig. 1B, i, iii), and 2.15 ± 0.24 *vs* 0.01 ± 0.01 copies μL^{-1}, $P < 0.001$, respectively (Fig. 1B,

https://doi.org/10.1017/S0031182022000610 Published online by Cambridge University Press

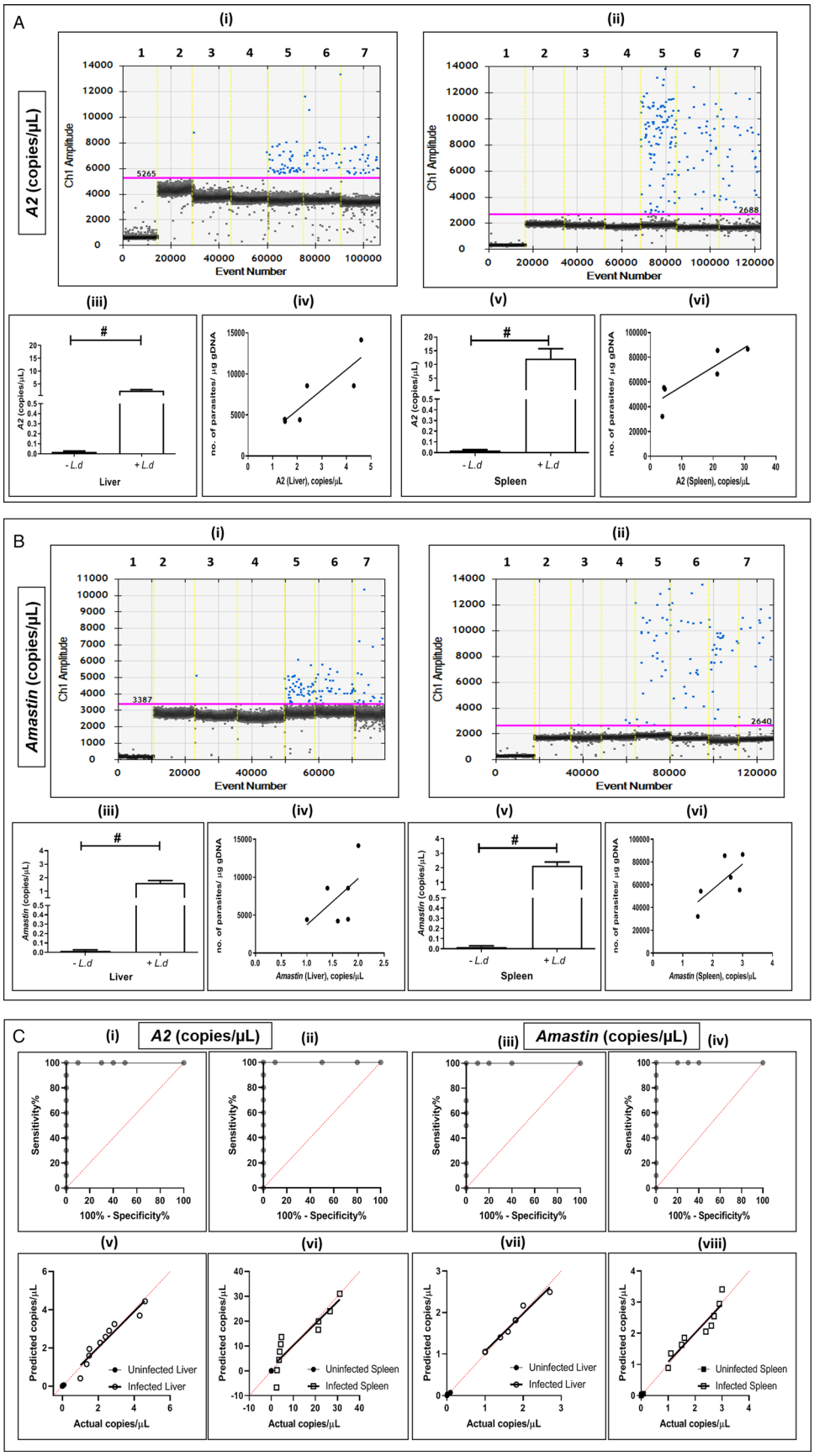

Fig. 1. Status of *A2* and *amastin* in hepatic and splenic tissues of infected Syrian golden hamsters. (A, B. i–ii) Representative 1-dimensional plots of droplets measured for fluorescence signals (amplitude indicated on *y*-axis) emitted from *A2* (A) and *amastin* (B) in infected ($n = 10$) and non-infected ($n = 10$) liver and splenic tissues of hamsters. Lane 1: negative controls; lane 2: non-template controls; lanes 3–4: non-infected liver and non-infected splenic tissues; lanes 5–7: infected hepatic (i) and splenic tissues (ii) respectively. EvaGreen-bound positive droplets are shown in blue while negative droplets are shown in black, with expression of the genes quantified as copies per μL. (A, B. iii, v) Bar graphs showing mRNA expression of *A2* (A) and *amastin* (B) in infected hepatic (iii) and splenic tissues (v) of hamsters. Each horizontal bar represents mean ± S.E.M. of 10 animals in duplicates. $^{\#}P < 0.001$ as compared to uninfected counterparts. (A, B. iv, vi) Correlation between no. of parasites per μg gDNA with expression of *A2* (A) and *amastin* (B) in infected liver tissues (iv) and splenic tissues (vi) respectively; (C) receiver operating characteristic (ROC) curve for *A2* and *amastin* in hamster liver (i, iii) and splenic (ii, iv) tissues. Linear regression between predicted and actual ddPCR output (copies per μL) was observed for all tested targets and measured as R^2 in hamster liver (v, vii) and splenic (vi, viii) tissues.

https://doi.org/10.1017/S0031182022000610 Published online by Cambridge University Press

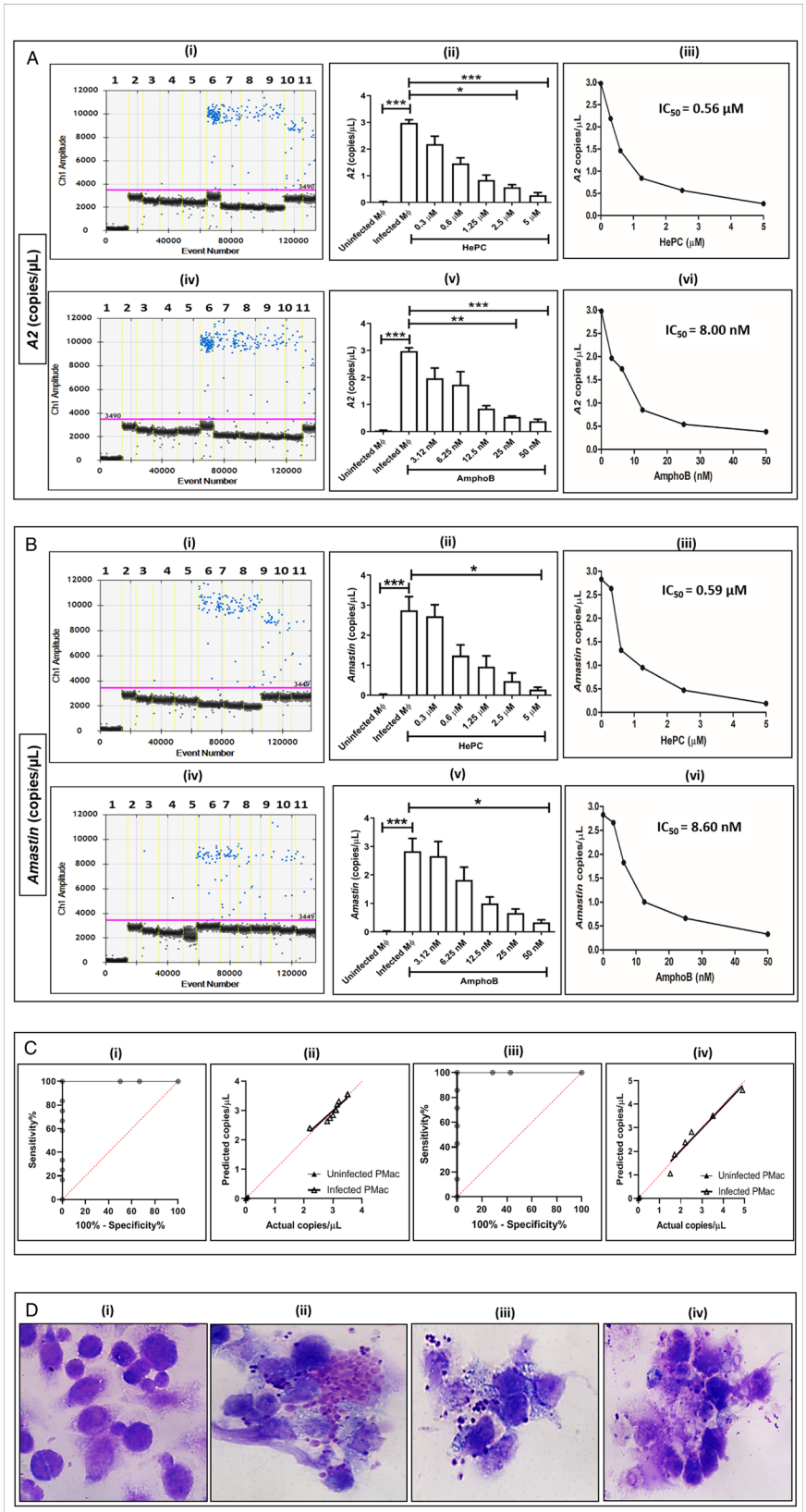

Fig. 2. Status of *A2* (A) and *amastin* (B) in *L. donovani*-infected murine peritoneal macrophages. (A, B. i, iv) Representative 1-dimensional plots of droplets measured for fluorescence signals (amplitude indicated on *y*-axis) emitted from *A2* (A) and *amastin* (B) in murine peritoneal macrophages infected with *L. donovani* followed by treatment with HePC (i) or AmphoB (iv) as described in Materials and methods section. Lane 1: negative control, lane 2: non-template control, lanes 3, 4: log phase and stationary phase promastigotes respectively, lane 5: control, non-infected peritoneal macrophages, lane 6: infected peritoneal macrophages, lanes 7–11: HePC (0.3–5 μM) [i] and AmphoB (3.12–50 nM) [iv] treated peritoneal macrophages. EvaGreen-bound positive droplets are shown in blue while negative droplets are shown in black, with expression of the genes quantified as the copies per μL. (A, B. ii, v) Bar graphs showing mRNA expression of *A2* (A) and *amastin* (B) in peritoneal macrophages infected with *L. donovani* and treated with HePC (ii) or Ampho B (v). Each horizontal bar represents mean ± S.E.M. of at least 3 different experiments in duplicates; $^{*}P < 0.05$, $^{**}P < 0.01$ and $^{***}P < 0.001$ as compared to infected macrophages. (A, B. iii, vi) Anti-amastigote activities of HePC (iii) and AmphoB (vi) were evaluated as described in Materials and methods section. (C) Receiver operating characteristic (ROC) curve for *A2* (i) and *amastin* (iii) in infected peritoneal macrophages. Linear regression between predicted and actual ddPCR output (copies per μL) was observed for *A2* (ii) and *amastin* (iv). (D) Representative images showing the anti-amastigote activity of HePC and AmphoB in AG83-infected peritoneal macrophages. Murine peritoneal macrophages (i) infected with *L. donovani* promastigotes (ii) treated with 0.6 μM HePC (iii) or 12.5 nM AmphoB (iv); Bar-10 μm, magnification 1000×.

ii, v). There was a robust positive correlation with hepatic ($r = 0.56$) and splenic parasite load ($r = 0.68$, Fig. 1B, iv, vi).

Assay specificity and sensitivity

The assay specificity was confirmed using cDNA from target sources (amastigotes in experimental models or dermal lesions from patients with PKDL) while non-target samples included promastigotes, uninfected hamster tissues and peritoneal macrophages along with skin biopsies from healthy individuals. The control arms exhibited the expression of *A2* and *amastin* similar to NTC. The LOQ was equivalent to LOD and for both *A2* and *amastin* was 0.15 copies μL^{-1}. AUC for *A2* and *amastin* in the liver (Fig. 1C, i, iii) and the spleen (Fig. 1C, ii, iv) was 1.000 (95% CI); R^2 for

https://doi.org/10.1017/S0031182022000610 Published online by Cambridge University Press

Table 1. Study population

Characteristics	Patients with PKDL ($n = 10$)	Healthy controls ($n = 10$)
Age (years)[a]	21.50 (16.50–43.75)	3.05 (1.05–5.57)
Sex (male: female)	2:3	Only males
Lesion type (macular: polymorphic)	2:3	NA
Disease duration (years)[a]	2.00 (0.95–4.50)	NA
Lag period (interval between cure of VL and onset of PKDL, years)[a]	3.00 (1.00–5.50)	NA
ITS-1 PCR +ve	10/10, 100%	NA
Parasite load (parasites per μg of genomic DNA)[a]	6652 (3896–28, 556)	NA

ITS-1 PCR, internal transcribed spacer-1 polymerase chain reaction; NA, not applicable; PKDL, post kala-azar dermal leishmaniasis; VL, visceral leishmaniasis.
[a]Values given in median (IQR).

A2 in the liver and the spleen was 0.91 and 0.80, while for *amastin*, it was 0.97 and 0.89, respectively (Fig. 1C, v–viii).

Measurement of amastigote-specific genes A2 and amastin in Leishmania-infected peritoneal macrophages

In an *ex vivo* model of infection wherein murine peritoneal macrophages were infected with stationary phase promastigotes, *A2* was enhanced as compared to uninfected macrophages, being 2.97 ± 0.12 *vs* 0.02 ± 0.01 copies μL^{-1}, $P < 0.001$ (Fig. 2A). Importantly, *A2* in log and stationary phase promastigotes (AG83) was comparable with NTC, confirming assay specificity. HePC/miltefosine caused a dose-dependent decrease in *A2* from 2.97 ± 0.12 to 2.18 ± 0.29 (0.3 μM), 1.46 ± 0.20 (0.6 μM), 0.84 ± 0.18 (1.25 μM), 0.57 ?? 0.09 ($P < 0.05$, 2.5 μM) and 0.27 ± 0.10 copies μL^{-1} ($P < 0.001$, 5 μM) and the IC_{50} was graphically extrapolated to be 0.56 μM (Fig. 2A, i–iii). Similarly, AmphoB caused a progressive dose-dependent decrease in *A2* from 2.97 ± 0.12 to 1.96 ± 0.38 (3.12 nM), 1.74 ± 0.48 (6.25 nM), 0.85 ± 0.10 (12.5 nM), 0.54 ± 0.03 ($P < 0.01$, 25.0 nM) and 0.38 ± 0.07 copies μL^{-1} ($P < 0.001$, 50 nM) and the IC_{50} was 8.0 nM (Fig. 2A, iv–vi).

Similarly, *amastin* was significantly raised in infected macrophages as compared to their non-infected counterparts, being 2.82 ± 0.45 *vs* 0.02 ± 0.01 copies μL^{-1}, $P < 0.001$ (Fig. 2B), whereas in log and stationary phase promastigotes, it remained similar to NTC, corroborating assay specificity. HePC caused a dose-dependent decrease in *amastin* from 2.82 ± 0.45 to 2.63 ± 0.38 (0.3 μM), 1.32 ± 0.35 (0.6 μM), 0.95 ± 0.35 (1.25 μM), 0.47 ± 0.27 (2.5 μM) and 0.18 ± 0.08 copies μL^{-1} ($P < 0.05$, 5 μM, Fig. 2B, i–iii), the derived IC_{50} being 0.59 μM. Similarly, AmphoB demonstrated a dose-dependent decrease being 2.82 ± 0.45, 2.66 ± 0.51 (3.12 nM), 1.82 ± 0.44 (6.25 nM), 1.00 ± 0.22 (12.5 nM), 0.66 ± 0.14 (25 nM) and 0.32 ± 0.09 copies μL^{-1} ($P < 0.05$, 50 nM), and the IC_{50} extrapolated was 8.6 nM (Fig. 2B, iv–vi).

For *A2* and *amastin*, AUC was 1.000 (95% CI), $P < 0.0001$ (Fig. 2C, i, iii); R^2 for *A2* and *amastin* in infected peritoneal macrophages was 0.90 and 0.95, respectively (Fig. 2C, ii, iv). In parallel, Giemsa-stained macrophages were microscopically examined (Fig. 2D), and the IC_{50} of HePC and AmphoB was 0.62 μM and 8.4 nM, respectively.

Measurement of amastigote-specific genes in patients with post kala-azar dermal leishmaniasis

This study objectively quantified the parasite burden in skin lesions sourced from patients with PKDL (Table 1). In PKDL, *A2* was significantly enhanced in PKDL cases with respect to healthy controls, being 9.22 ± 1.34 *vs* 0.03 ± 0.00 copies μL^{-1} respectively, $P < 0.001$ (Fig. 3A, i–iii) as was *amastin*, 5.17 ± 0.64 *vs* 0.03 ± 0.01 copies μL^{-1}, $P < 0.001$, respectively (Fig. 3B, i–iii). Both *A2* and *amastin* correlated positively with parasite load, $r = 0.91$ and $r = 0.82$, respectively (Fig. 3A, B, iv). The AUC is 1.000 (95% CI 1.000–1.000) for *A2* (Fig. 3C, i) and *amastin* (Fig. 3C, iii) and the R^2 for *A2* and *amastin* was 0.98 and 0.97, respectively (Fig. 3C, ii, iv).

Discussion

Distinct morphological and biochemical changes occur during the differentiation of promastigotes into infective amastigotes (Holst-Jensen *et al.*, 2003; Pinheiro *et al.*, 2012). In view of *A2* and *amastin* being exclusively present in amastigotes, it suggested their critical role in supporting parasite survival within host macrophages. Parasites like *T. cruzi* or *Leptomonas* are expected to demonstrate positivity, but *amastin* is more abundant in *Leishmania* spp. (Jackson, 2010). To obviate this cross-reactivity, the primers used in this study were exclusively designed for *Leishmania* spp. and therefore would not show any amplification for other parasites. The initial standardization for *A2* and *amastin* endorsed the potential of ddPCR to monitor parasite load, and also emphasized that the optimal concentration of template was important (Supplementary Table S1 and Figs S2–S4). Moreover, their positive correlation with kDNA in qPCR and statistically evaluated AUC values established the assay sensitivity (Fig. 1). Importantly, as the non-target samples yielded a negative amplicon for *A2* and *amastin*, it unequivocally confirmed assay specificity. Furthermore, the stage-specific expression of *A2* and *amastin* was validated by its negative expression in promastigotes, and with the establishment of infection and transformation into amastigotes, it clearly correlated with an enhanced expression of *A2* and *amastin* (Fig. 2).

Drug development in leishmaniasis till date depends on the quantification of amastigotes in *ex vivo*-infected macrophages, the classical method being counting of Giemsa-stained macrophages. However, this approach has an inherent operator bias, is time consuming and laborious, and cannot be applied for high-throughput screening. This limitation can be circumvented by employing objective approaches, e.g. kDNA-based qPCR. This is feasible within an established animal model of *Leishmania* infection wherein the expression of amastigotes can be quantified in terms of kDNA on the assumption that only amastigotes are present (Moulik *et al.*, 2021*a*). However, in short-term *ex vivo* drug screening methods as in peritoneal macrophages, quantification by kDNA qPCR approach maybe inadequate as despite numerous washing steps, a substantial proportion of promastigotes can remain loosely adherent to macrophages and would result in a false positivity. This can be obviated if quantification of amastigotes with *A2* and *amastin* is adopted. Additionally, detection by ddPCR eliminated the need for standard curves for *A2* and *amastin*. The generation of amastigotes *in vitro* would be needed to create a standard curve for qPCR but this is not feasible. Also, quantifying the precise number of amastigotes in *Leishmania*-infected peritoneal macrophages cannot be tailor-made for standard curve as the degree of infectivity can vary. Therefore, in this light, this ddPCR approach has a strong potential to be translated into a high-throughput drug screening platform. In view of the IC_{50} of miltefosine (HePC) and amphotericin B (AmphoB) in parasitized macrophages, as measured by conventional microscopy matching with the IC_{50} quantitatively determined by ddPCR (Fig. 2A–D), it endorsed the implementation of ddPCR.

Patients with PKDL can present with papulonodular (polymorphic) or hypomelanotic lesions (macular). These cases are

https://doi.org/10.1017/S0031182022000610 Published online by Cambridge University Press

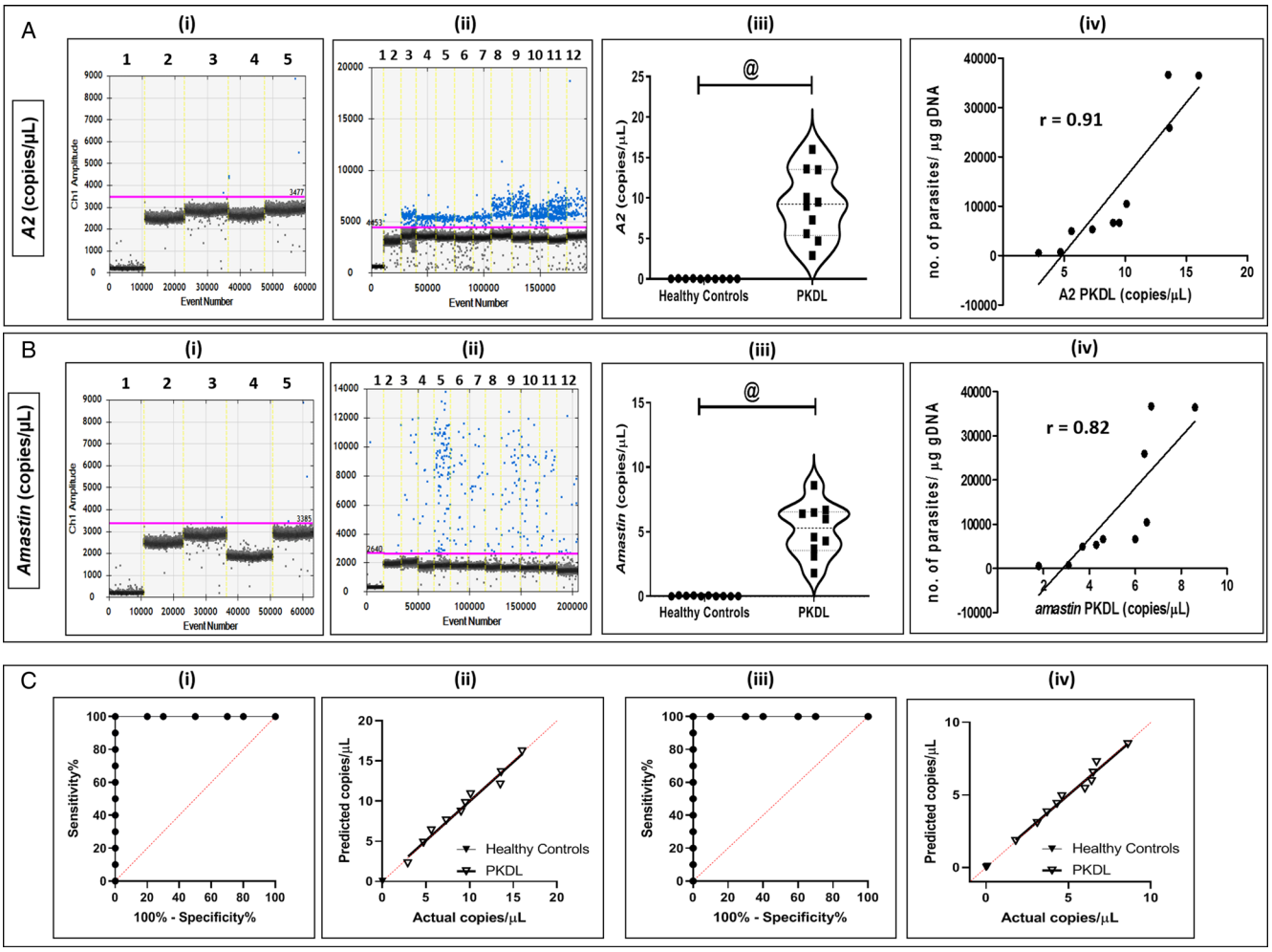

Fig. 3. Status of amastigote-specific genes *A2* (A) and *amastin* (B) in PKDL. (A, B) Representative 1-dimensional plots of droplets measured for fluorescence signals (amplitude indicated on y-axis) emitted from *A2* (A) and *amastin* (B) in skin biopsies sourced from PKDL cases ($n = 10$) and healthy controls ($n = 10$). EvaGreen-bound positive droplets are shown in blue while negative droplets are shown in black, with expression of genes quantified as copies per μL. (i) Lane 1: negative controls, lane 2: non-template controls, lanes 3–5: healthy controls for *A2* (A) and *Amastin* (B) respectively. (ii) Lane 1: negative controls, lane 2: non-template controls, lanes 3–12: PKDL cases tested for expression of *A2* (A) and *Amastin* (B) respectively. (iii) Violin plots showing mRNA expression of *A2* (A) and *amastin* (B) in PKDL cases and healthy controls ($n = 10$). Each horizontal bar represents mean ± S.E.M. of 10 individuals in duplicates; $^{@}P < 0.001$ as compared to healthy controls. (iv) Correlation between number of parasites per μg gDNA with *A2* (A) and *amastin* (B) in PKDL cases. (C) Receiver operating characteristic (ROC) curve for *A2* (i) and *amastin* (iii) in PKDL cases. Linear regression between predicted and actual ddPCR output (copies per μL) was observed for all tested targets in PKDL for *A2* (ii) and *amastin* (iv).

considered as the disease reservoir, especially during inter-epidemic periods, and therefore have an immense epidemiological significance (de Paiva *et al.*, 2015; Zijlstra *et al.*, 2017; Gedda *et al.*, 2020). Sero-diagnostics for kala-azar/VL involves ELISA-based assays employing crude or soluble antigens sourced from *Leishmania* spp. and rK39-immunochromatographic test is the most robust assay (Saha *et al.*, 2005; Sundar *et al.*, 2006; Mondal *et al.*, 2019). Additionally, the heightened anti-leishmanial IgG and its subclasses have helped identify and monitor active VL and PKDL cases (Mukhopadhyay *et al.*, 2012; Bhattacharyya *et al.*, 2014; Sengupta and Chatterjee, 2021). Other important *Leishmania*-specific antigens include recombinant GP63, recombinant cysteine protease A (Didwania *et al.*, 2020) and *Leishmania* membrane antigen (Ejazi *et al.*, 2019). Alternatively, antigen detection in urine can be expected to broadly correlate with the parasite load (Ejazi *et al.*, 2016). The A2 amastigote antigen-based LAT was performed in VL cases (Akhoundi *et al.*, 2013), but no similar study has been performed to identify PKDL cases.

A major limitation in the diagnosis of PKDL is that (a) serological tests are of limited value as positivity can be attributed to a past episode of VL and (b) detection of parasites in Giemsa-stained skin biopsies is a major challenge especially for macular PKDL which presently constitute almost 50% of the PKDL disease burden (Sengupta *et al.*, 2019). Additionally, the limited availability of a standardized 'test of cure' tool for guiding clinicians is a major limitation, as till date the resolution of clinical features is considered as the efficacy parameter. Therefore, this study may find value in PKDL-related clinical trials, an area where chemotherapy regimens till date remain empirical.

Interestingly, *A2* has been implicated only in visceralization during establishment of infection, and was considered to be selectively expressed in VL, with negligible expression in CL and PKDL lesions (Sharma *et al.*, 2010). However, as this study has demonstrated the presence of *A2* and *amastin* in PKDL (Fig. 3), it may be attributed to a lower sensitivity of the assay employed in that study *vis-a-vis* the more sensitive ddPCR used in this study. The presence of *A2* in PKDL has opened new avenues in understanding the potential dermatotropic role of *A2* in the pathogenesis of PKDL (Fig. 3). Also, it would be interesting to study the effectiveness of using *A2* as a monitoring tool for CL, where interpretation of lesion healing is challenging.

Overall, the optimized ddPCR assay was demonstrated to be sensitive as the linear regression curves exhibited strong goodness

https://doi.org/10.1017/S0031182022000610 Published online by Cambridge University Press

of fit. However, the reagents and ddPCR machines are expensive and perhaps difficult to use as a common tool in laboratories. Irrespective of the study models, the expression of *A2* was consistently greater than *amastin*, and would be the preferred biomarker in future. The availability of such a molecular diagnostic platform involving precise detection of amastigote burden will be an invaluable asset for drug screening as also for conducting clinical trials, and thus provide strong support for the ongoing leishmaniasis elimination programme in South Asia.

Supplementary material. The supplementary material for this article can be found at https://doi.org/10.1017/S0031182022000610.

Acknowledgements. The work received technical support from the Multidisciplinary Research Unit (MRU), IPGME&R (V.25011/103/2016-HR).

Author contributions. M. R., D. S. and M. C. conceived and designed the study. M. R. and D. S. conducted data gathering. M. R. performed statistical analyses. M. R. and M. C. wrote the article.

Financial support. The work received financial assistance from the Department of Science and Technology, Government of West Bengal [grant number 969/(Sanc)/ST/P/SandT/9G-22/2016], Indian Council of Medical Research (ICMR) Government of India [grant numbers: 6/9-7(151)2017-ECD II and 6/9-7(263)KA/2021/ECD II], JC Bose Fellowship, Science & Engineering Board, Government of India (JCB/2019/000043). M. R. and D. S. are recipients of Senior Research Fellowship from University Grants Commission and ICMR, Government of India, respectively. The funders had no role in study design, data collection and analysis, decision to publish or preparation of the manuscript.

Conflict of interest. None.

Ethical standards. All animal-related experiments were approved by the Institutional Animal Ethics Committee of IPGME&R, Kolkata (CPCSEA Registration No. 544/PO/c/02/CPCSEA). All human-related work included repurposed DNA after receiving approval from the Institutional Ethics Committee of School of Tropical Medicine, Kolkata and Institute of Post Graduate Medical Education and Research (IPGME&R), Kolkata. Written informed consent was obtained from all individuals, and for a minor, their legally accepted representative provided the same.

References

Abbasi I, Aramin S, Hailu A, Shiferaw W, Kassahun A, Belay S, Jaffe C and Warburg A (2013) Evaluation of PCR procedures for detecting and quantifying *Leishmania donovani* DNA in large numbers of dried human blood samples from a visceral leishmaniasis focus in Northern Ethiopia. *BMC Infectious Diseases* **13**, 153.

Akhoundi B, Mohebali M, Shojaee S, Jalali M, Kazemi B, Bandehpour M, Keshavarz H, Edrissian GH, Eslami MB, Malekafzali H and Kouchaki A (2013) Rapid detection of human and canine visceral leishmaniasis: assessment of a latex agglutination test based on the A2 antigen from amastigote forms of *Leishmania infantum*. *Experimental Parasitology* **133**, 307–313.

Avishek K, Ahuja K, Pradhan D, Gannavaram S, Selvapandiyan A, Nakhasi HL and Salotra P (2018) A leishmania-specific gene upregulated at the amastigote stage is crucial for parasite survival. *Parasitology Research* **117**, 3215–3228.

Bates PA (2018) Revising *Leishmania's* life cycle. *Nature Microbiology* **3**, 529–530.

Belmonte FR, Martin JL, Frescura K, Damas J, Pereira F, Tarnopolsky MA and Kaufman BA (2016) Digital PCR methods improve detection sensitivity and measurement precision of low abundance mtDNA deletions. *Scientific Reports* **6**, 25186.

Bhattacharyya T, Ayandeh A, Falconar AK, Sundar S, El-Safi S, Gripenberg MA, Bowes DE, Thunissen C, Singh OP, Kumar R, Ahmed O, Eisa O, Saad A, Silva Pereira S, Boelaert M, Mertens P and Miles MA (2014) IgG1 as a potential biomarker of post-chemotherapeutic relapse in visceral leishmaniasis, and adaptation to a rapid diagnostic test. *PLoS Neglected Tropical Diseases* **8**, e3273.

Cai Y, Li X, Lv R, Yang J, Li J, He Y and Pan L (2014) Quantitative analysis of pork and chicken products by droplet digital PCR. *Biomed Research International* **2014**, 810209.

Carvalho FA, Charest H, Tavares CA, Matlashewski G, Valente EP, Rabello A, Gazzinelli RT and Fernandes AP (2002) Diagnosis of American visceral leishmaniasis in humans and dogs using the recombinant *Leishmania donovani* A2 antigen. *Diagnostic Microbiology and Infectious Disease* **43**, 289–295.

Chappuis F, Sundar S, Hailu A, Ghalib H, Rijal S, Peeling RW, Alvar J and Boelaert M (2007) Visceral leishmaniasis: what are the needs for diagnosis, treatment and control? *Nature Reviews. Microbiology* **5**, 873–882.

Charest H and Matlashewski G (1994) Developmental gene expression in *Leishmania donovani:* differential cloning and analysis of an amastigote-stage-specific gene. *Molecular and Cellular Biology* **14**, 2975–2984.

de Paiva RM, Grazielle-Silva V, Cardoso MS, Nakagaki BN, Mendonça-Neto RP, Canavaci AM, Souza Melo N, Martinelli PM, Fernandes AP, daRocha WD and Teixeira SM (2015) Amastin knockdown in *Leishmania braziliensis* affects parasite-macrophage interaction and results in impaired viability of intracellular amastigotes. *PLoS Pathogens* **11**, e1005296.

Didwania N, Ejazi SA, Chhajer R, Sabur A, Mazumder S, Kamran M, Kar R, Pandey K, Das V, Das P, Rahaman M, Goswami RP and Ali N (2020) Evaluation of cysteine protease C of *Leishmania donovani* in comparison with glycoprotein 63 and elongation factor 1α for diagnosis of human visceral leishmaniasis and for posttreatment follow-up response. *Journal of Clinical Microbiology* **58**, e00213–20.

Dighal A, Mukhopadhyay D, Sengupta R, Moulik S, Mukherjee S, Roy S, Chaudhuri SJ, Das NK and Chatterjee M (2020) Iron trafficking in patients with Indian post kala-azar dermal leishmaniasis. *PLoS Neglected Tropical Diseases* **14**, e0007991.

Ejazi SA, Bhattacharya P, Bakhteyar MA, Mumtaz AA, Pandey K, Das VN, Das P, Rahaman M, Goswami RP and Ali N (2016) Noninvasive diagnosis of visceral leishmaniasis: development and evaluation of two urine-based immunoassays for detection of *Leishmania donovani* infection in India. *PLoS Neglected Tropical Diseases* **10**, e0005035.

Ejazi SA, Ghosh S, Saha S, Choudhury ST, Bhattacharyya A, Chatterjee M, Pandey K, Das VNR, Das P, Rahaman M, Goswami RP, Rai K, Khanal B, Bhattarai NR, Deepachandi B, Siriwardana YD, Karunaweera ND, deBrito MEF, Gomes YM, Nakazawa M, Costa CHN, Adem E, Yeshanew A, Melkamu R, Fikre H, Hurissa Z, Diro E, Carrillo E, Moreno J and Ali N (2019) A multicentric evaluation of dipstick test for serodiagnosis of visceral leishmaniasis in India, Nepal, Sri Lanka, Brazil, Ethiopia and Spain. *Scientific Reports* **9**, 9932.

Escobar P, Matu S, Marques C and Croft SL (2002) Sensitivities of *Leishmania* species to hexadecylphosphocholine (miltefosine), ET-18–OCH(3) (edelfosine) and amphotericin B. *Acta Tropica* **81**, 151–157.

Floren C, Wiedemann I, Brenig B, Schütz E and Beck J (2015) Species identification and quantification in meat and meat products using droplet digital PCR (ddPCR). *Food Chemistry* **173**, 1054–1058.

Garg R and Dube A (2006) Animal models for vaccine studies for visceral leishmaniasis. *The Indian Journal of Medical Research* **123**, 439–454.

Gedda MR, Singh B, Kumar D, Singh AK, Madhukar P, Upadhyay S, Singh OP and Sundar S (2020) Post kala-azar dermal leishmaniasis: a threat to elimination program. *PLoS Neglected Tropical Diseases* **14**, e0008221.

Ghosh S, Das NK, Mukherjee S, Mukhopadhyay D, Barbhuiya JN, Hazra A and Chatterjee M (2015) Inadequacy of 12-week miltefosine treatment for Indian post-kala-azar dermal leishmaniasis. *The American Journal of Tropical Medicine and Hygiene* **93**, 767–769.

Gobert G, Cotillard A, Fourmestraux C, Pruvost L, Miguet J and Boyer M (2018) Droplet digital PCR improves absolute quantification of viable lactic acid bacteria in faecal samples. *Journal of Microbiological Methods* **148**, 64–73.

Holst-Jensen A, Rønning SB, Løvseth A and Berdal KG (2003) PCR technology for screening and quantification of genetically modified organisms (GMOs). *Analytical and Bioanalytical Chemistry* **375**, 985–993.

Hossain F, Ghosh P, Khan M, Duthie MS, Vallur AC, Picone A, Howard RF, Reed SG and Mondal D (2017) Real-time PCR in detection and quantitation of *Leishmania donovani* for the diagnosis of visceral leishmaniasis patients and the monitoring of their response to treatment. *PLoS ONE* **12**, e0185606.

Jackson AP (2010) The evolution of amastin surface glycoproteins in trypanosomatid parasites. *Molecular Biology and Evolution* **27**, 33–45.

Johnston DA, Blaxter ML, Degrave WM, Foster J, Ivens AC and Melville SE (1999) Genomics and the biology of parasites. *Bioessays: News and Reviews in Molecular, Cellular and Developmental Biology* **21**, 131–147.

Karmakar J, Roy S and Mandal C (2019) Modulation of TLR4 sialylation mediated by a Sialidase Neu1 and impairment of its signaling in *Leishmania donovani* infected macrophages. *Frontiers in Immunology* **10**, 2360.

Mary C, Faraut F, Lascombe L and Dumon H (2004) Quantification of *Leishmania infantum* DNA by a real-time PCR assay with high sensitivity. *Journal of Clinical Microbiology* **42**, 5249–5255.

Mary C, Faraut F, Drogoul MP, Xeridat B, Schleinitz N, Cuisenier B and Dumon H (2006) Reference values for *Leishmania infantum* parasitemia in different clinical presentations: quantitative polymerase chain reaction for therapeutic monitoring and patient follow-up. *The American Journal of Tropical Medicine and Hygiene* **75**, 858–863.

Matlashewski G (2001) *Leishmania* infection and virulence. *Medical Microbiology and Immunology* **190**, 37–42.

McCall LI and Matlashewski G (2010) Localization and induction of the A2 virulence factor in *Leishmania*: evidence that A2 is a stress response protein. *Molecular Microbiology* **77**, 518–530.

Melby PC, Chandrasekar B, Zhao W and Coe JE (2001) The hamster as a model of human visceral leishmaniasis: progressive disease and impaired generation of nitric oxide in the face of a prominent Th1-like cytokine response. *Journal of Immunology* **166**, 1912–1920.

Mondal D, Bern C, Ghosh D, Rashid M, Molina R, Chowdhury R, Nath R, Ghosh P, Chapman L, Alim A, Bilbe G and Alvar J (2019) Quantifying the infectiousness of post-kala-azar dermal leishmaniasis toward sand flies. *Clinical Infectious Diseases* **69**, 251–258.

Moreira ND, Vitoriano-Souza J, Roatt BM, Vieira PM, Ker HG, de Oliveira Cardoso JM, Giunchetti RC, Carneiro CM, de Lana M and Reis AB (2012) Parasite burden in hamsters infected with two different strains of leishmania (*Leishmania*) *infantum*: 'Leishman Donovan units' versus real-time PCR. *PLoS ONE* **7**, e47907.

Moulik S, Chaudhuri SJ, Sardar B, Ghosh M, Saha B, Das NK and Chatterjee M (2018) Monitoring of parasite kinetics in Indian post-kala-azar dermal leishmaniasis. *Clinical Infectious Diseases* **66**, 404–410.

Moulik S, Karmakar J, Joshi S, Dube A, Mandal C and Chatterjee M (2021a) Status of IL-4 and IL-10 driven markers in experimental models of visceral leishmaniasis. *Parasite Immunology* **43**, e12783.

Moulik S, Sengupta S and Chatterjee M (2021b) Molecular tracking of the *Leishmania* parasite. *Frontiers in Cellular and Infection Microbiology* **11**, 623437.

Mukhopadhyay D, Das NK, De Sarkar S, Manna A, Ganguly DN, Barbhuiya JN, Maitra AK, Hazra A and Chatterjee M (2012) Evaluation of serological markers to monitor the disease status of Indian post kala-azar dermal leishmaniasis. *Transactions of the Royal Society of Tropical Medicine and Hygiene* **106**, 668–676.

Pinheiro LB, Coleman VA, Hindson CM, Herrmann J, Hindson BJ, Bhat S and Emslie KR (2012) Evaluation of a droplet digital polymerase chain reaction format for DNA copy number quantification. *Analytical Chemistry* **84**, 1003–1011.

Rafati S, Hassani N, Taslimi Y, Movassagh H, Rochette A and Papadopoulou B (2006) Amastin peptide-binding antibodies as biomarkers of active human visceral leishmaniasis. *Clinical and Vaccine Immunology* **13**, 1104–1110.

Rochette A, McNicoll F, Girard J, Breton M, Leblanc E, Bergeron MG and Papadopoulou B (2005) Characterization and developmental gene regulation of a large gene family encoding amastin surface proteins in *Leishmania* spp. *Molecular and Biochemical Parasitology* **140**, 205–220.

Saha S, Mazumdar T, Anam K, Ravindran R, Bairagi B, Saha B, Goswami R, Pramanik N, Guha SK, Kar S, Banerjee D and Ali N (2005) *Leishmania* promastigote membrane antigen-based enzyme-linked immunosorbent assay and immunoblotting for differential diagnosis of Indian post-kala-azar dermal leishmaniasis. *Journal of Clinical Microbiology* **43**, 1269–1277.

Saini S and Rai AK (2020) Hamster, a close model for visceral leishmaniasis: opportunities and challenges. *Parasite Immunology* **42**, e12768.

Salotra P, Sreenivas G, Pogue GP, Lee N, Nakhasi HL, Ramesh V and Negi NS (2001) Development of a species-specific PCR assay for detection of *Leishmania donovani* in clinical samples from patients with kala-azar and post-kala-azar dermal leishmaniasis. *Journal of Clinical Microbiology* **39**, 849–854.

Sengupta S and Chatterjee M (2021) IgG3 and IL10 are effective biomarkers for monitoring therapeutic effectiveness in post kala-azar dermal leishmaniasis. *PLoS Neglected Tropical Diseases* **15**, e0009906.

Sengupta R, Chaudhuri SJ, Moulik S, Ghosh MK, Saha B, Das NK and Chatterjee M (2019) Active surveillance identified a neglected burden of macular cases of post kala-azar dermal leishmaniasis in West Bengal. *PLoS Neglected Tropical Diseases* **13**, e0007249.

Sharma P, Gurumurthy S, Duncan R, Nakhasi HL and Salotra P (2010) Comparative in vivo expression of amastigote up regulated *Leishmania* genes in three different forms of leishmaniasis. *Parasitology International* **59**, 262–264.

Sudarshan M, Weirather JL, Wilson ME and Sundar S (2011) Study of parasite kinetics with antileishmanial drugs using real-time quantitative PCR in Indian visceral leishmaniasis. *The Journal of Antimicrobial Chemotherapy* **66**, 1751–1755.

Sundar S, Singh RK, Maurya R, Kumar B, Chhabra A, Singh V and Rai M (2006) Serological diagnosis of Indian visceral leishmaniasis: direct agglutination test versus rK39 strip test. *Transactions of the Royal Society of Tropical Medicine and Hygiene* **100**, 533–537.

Sunter J and Gull K (2017) Shape, form, function and *Leishmania* pathogenicity: from textbook descriptions to biological understanding. *Open Biology* **7**, 170165.

Verma S, Kumar R, Katara GK, Singh LC, Negi NS, Ramesh V and Salotra P (2010) Quantification of parasite load in clinical samples of leishmaniasis patients: IL-10 level correlates with parasite load in visceral leishmaniasis. *PLoS ONE* **5**, e10107.

Vermeersch M, da Luz RI, Toté K, Timmermans JP, Cos P and Maes L (2009) In vitro susceptibilities of *Leishmania donovani* promastigote and amastigote stages to antileishmanial reference drugs: practical relevance of stage-specific differences. *Antimicrobial Agents and Chemotherapy* **53**, 3855–3859.

Yardley V, Croft SL, De Doncker S, Dujardin JC, Koirala S, Rijal S, Miranda C, Llanos-Cuentas A and Chappuis F (2005) The sensitivity of clinical isolates of *Leishmania* from Peru and Nepal to miltefosine. *The American Journal of Tropical Medicine and Hygiene* **73**, 272–275.

Zijlstra EE, Alves F, Rijal S, Arana B and Alvar J (2017) Post-kala-azar dermal leishmaniasis in the Indian subcontinent: a threat to the South-East Asia region kala-azar elimination programme. *PLoS Neglected Tropical Diseases* **11**, e0005877.

https://doi.org/10.1017/S0031182022000610 Published online by Cambridge University Press